UNSW SYDNEY

Structural, Optical and Phonon properties of hafnium oxynitride thin films synthesized using plasma-enhanced atomic layer deposition

Author:
Pratik, Ayush; Patterson, Robert; Conibeer, Gavin; Shrestha, Santosh

Publication details:
Journal of Alloys and Compounds
v. 983
pp. 173925 - 173925
0925-8388 (ISSN)

Publication Date:
2024-02

Publisher DOI:
https://doi.org/10.1016/j.jallcom.2024.173925

License:
https://creativecommons.org/licenses/by/4.0/
Link to license to see what you are allowed to do with this resource.

Downloaded from http://hdl.handle.net/1959.4/unsworks_85622 in https://unsworks.unsw.edu.au on 2024-05-18

Journal of Alloys and Compounds 983 (2024) 173925

Contents lists available at ScienceDirect

Journal of Alloys and Compounds

journal homepage: www.elsevier.com/locate/jalcom

Structural, optical and phonon properties of hafnium oxynitride thin films synthesized using plasma-enhanced atomic layer deposition

Ayush Pratik *, Robert Patterson, Gavin Conibeer, Santosh Shrestha

School of Photovoltaic and Renewable Energy Engineering, University of New South Wales, Sydney, NSW 2052, Australia

ARTICLE INFO

Keywords:
Hafnium oxynitride
Atomic layer deposition
Absorption coefficient
Hot carrier solar cells
Phonon bottleneck effect
Acoustic impedance

ABSTRACT

Hafnium Oxynitride belongs to the group IVB compounds with high permittivity and large acoustic impedance. In this work, hafnium oxynitride films have been synthesized using plasma-enhanced atomic layer deposition on Si and Quartz substrates. XRD results show the presence of mixed cubic and monoclinic phases with an optimum crystallization occurring at 850 °C. The thin films show strong absorption in the UV–visible spectrum suggesting semiconductor behaviour. The optical properties of the spectrophotometer and spectroscopic ellipsometry agree with the XRD observations. We also report the first observation of experimentally derived photoluminescence (PL) from hafnium oxynitride thin films synthesized using plasma-enhanced atomic layer deposition. The PL spectrum is consistent with the XRD results with two absorption peaks around 576 nm and 705 nm, corresponding to cubic and monoclinic phases, respectively. Also, the PL results match very well with the theoretical value of the band gap of cubic and monoclinic phases of Hf_2ON_2. The Raman spectrum shows a phonon band gap around 242–263 cm^{-1}, consistent with the theoretically reported value for cubic Hf_2ON_2.

1. Introduction

Hafnium-based oxides and nitrides have found extensive applications such as in field-effect transistors, micro-electronics, and capacitors, primarily because of hafnium oxide's large permittivity (k). In some of the recent applications of CMOS, Hafnium-based compounds are seen as some of the best replacements for SiO_2 for increasing the capacitance at a desired thickness [1–4]. Hafnium oxynitride has also been studied as a catalyst for the reduction of oxygen in an acidic medium by doping HfO_2 with N_2 through hydrothermal treatments [5]. Hafnium oxynitride has also been synthesized in a perovskite structure to study the water-splitting activity under illumination. The hafnium oxynitride perovskites have been reported to have sufficient oxidation and reduction potential for water-splitting activity with semiconducting properties [6]. In most recent applications, hafnium oxynitride has also been studied from a hot carrier solar cell (HCSC) perspective where the thin films were synthesized using plasma-enhanced atomic layer deposition (PE-ALD) [7]. Similarly, hafnium nitride (HfN) has been studied extensively to study the absorber properties of HCSC [8–11]. The large phonon band gap and negligible electronic band gap give HfN the potential to exhibit the "Phonon Bottleneck Effect" (PBE), by which carrier thermalization is restricted by a limited ability for excited optical phonons to dissipate their energy [12–14]. The high acoustic impedance of 54.81 MRayl [$Kg/m^2/s$] gives Hafnium oxynitride an excellent potential to show the PBE as well. A material system with large acoustic impedance has a smaller acoustic phonon density of states, and thus offers a higher resistance to the decay of optical phonons and hence achieves a PBE at comparatively lower intensities compared to systems with a lower acoustic impedance. If this is coupled with a large phonon bandgap, then a strong restriction in optical phonon energy loss is likely.

High-quality nitrides are not easy to grow as they require ultrahigh vacuum systems to remove background oxygen and often involve very expensive processes [7,8,15]. Therefore, Hafnium oxynitride offers a good compromise for the nitrides as they are relatively easy to grow in good quality. The theoretical band gap of different phases of Hafnium oxynitride lies between 1.63 and 1.91 eV [16]. Also, the acoustic impedance of hafnium oxynitride is 54.81 MRayl which is only slightly lower than that for HfN (Z_{HfN} = 59 MRayl) but almost double that for InN (Z_{InN} = 35 MRayl), which has been suggested as an Ideal HCSC absorber [17–19].

Various research has been published on the synthesis and characterization of Hafnium oxynitride for potential applications as dielectrics and hot carrier solar cells. Young et. al. used NH_3 or N_2 plasma as reactants and tetrakis(dimethylamino)hafnium as Hf precursor to

* Corresponding author.
E-mail address: a.pratik@unsw.edu.au (A. Pratik).

https://doi.org/10.1016/j.jallcom.2024.173925
Received 6 November 2023; Received in revised form 22 January 2024; Accepted 19 February 2024
Available online 20 February 2024
0925-8388/© 2024 The Authors. Published by Elsevier B.V. This is an open access article under the CC BY license (http://creativecommons.org/licenses/by/4.0/).

synthesize Hafnium oxynitride through atomic layer deposition (ALD). They report an amorphous phase for the as-deposited films and an increase in the crystallization temperature after nitrogen incorporation as compared to the HfO_2 lattice. Nitrogen was uniformly distributed throughout the lattice of HfO_2 [20]. However, the films were insulating in behaviour and studied from a perspective of enhancement of dielectric constant and suppression of leakage current. We did not find any photoluminescence or optical study of the thin films. Jyun et al., synthesized Hafnium oxynitride to study its charge storage behaviour. They report sufficient and satisfactory charge retention properties and erase speeds of Hafnium oxynitride thin film. As-deposited films were amorphous in nature and crystallization was dependent both on the temperature and thickness of the films. Thin films of 2.5–5 nm hardly crystallized even at 900 ºC because of a lack of grain growth possibility in the z direction [21]. The Hafnium oxynitride thin film was not a single standing film but rather was sandwiched between Al_2O_3 and SiO_2. The Hafnium oxynitride film was reported to consist of 50% oxygen which likely makes it an oxide-rich rhombohedral phase with a large band gap. Bharat et. al. studied the structural and optical properties from an HCSC perspective and reported optimism for Hafnium oxynitride as an HCSC absorber. However, the deposited films were amorphous in nature with very high oxygen content. The authors report substantial absorption properties of the films with semiconducting behaviour [7]. However, we did not find detailed investigation into the phase analysis or materials behaviour in terms of optical, and semiconducting properties. The self-limiting reaction controls in the atomic layer deposition method have been an excellent advantage over sputtering processes, chemical & physical vapor deposition, spin coatings, and other thin film synthesis routes. The self-limiting behaviour ensures conformal film growth, precise thickness control of the films, and excellent repeatability of the process. Also, most of the hafnium oxynitride thin films reported in the literature have been synthesized by nitriding HfO_2 films through annealing in N_2 or NH_3 or oxidizing HfN films or sputtering [3,22–24]. These methods have mostly resulted in oxide-rich films with insulating properties. This is because the target property to study was from the perspective of Dielectrics which requires a large band gap and hence an oxide-rich phase. However, in this research, we aimed to synthesize the Hafnium Oxynitride thin films utilizing their semiconductor properties by controlling the background oxygen and increasing the N_2 plasma exposure. It is very difficult to remove all the background oxygen from the ALD chamber. So, the reactor was heated to the required temperature and purged with N_2 gas for more than 4 hours to reduce the background oxygen. We also hardly find any reports of Photoluminescence of Hafnium oxynitride thin films synthesized using plasma-assisted atomic layer deposition.

In this article, we report a detailed investigation of the structural, optical and phonon properties of Hafnium oxynitride thin films. This is the first report on experimentally derived PL emission spectra for plasma-assisted ALD-grown thin films of Hafnium oxynitride. We find a mixed cubic and monoclinic phase of hafnium oxynitride which is consistent with the theoretical values. The thin films are highly absorbing in the visible spectrum with absorption coefficients higher than those reported previously [7,15].

2. Materials and methods

Thin films of hafnium oxynitride were synthesised using tetrakis (ethylmethylamino)hafnium (TEMAHf) precursor as hafnium source, N_2 plasma (60 W) as nitrogen source and background oxygen in the ALD chamber as O_2 source. The amount of background oxygen in the chamber was controlled by adjusting the base pressure of the reactor. Thin hafnium oxynitride films were grown on RCA1 & RCA2 cleaned Si and Quartz substrates. The films were grown at a chamber temperature of 300 °C in a Beneq ALD TFS 200. The hafnium precursor was maintained at 100 °C using a hot source and was sent into the reaction chamber with a nitrogen flow of 35 sccm. The ALD cycle consisted of 0.2 s precursor pulse, 10 s nitrogen purge, 15 s nitrogen plasma and 10 s nitrogen purge sequentially. The as-deposited films were annealed using rapid thermal annealing (RTA) at temperatures from 800 to 900 °C for 15–120 s in a nitrogen atmosphere (Ramp rate = 40 °C/s). A few samples were subjected to standard furnace annealing abbreviated as “Anneal” 800 °C for 5 mins with a slow ramp rate of 1.5 ºC/s.

The thickness of the films was measured using a Dektak surface profiler and also by fitting to spectroscopic ellipsometry (SE) data. The refractive index, extinction coefficients and real & imaginary components of the dielectric constants were extracted by fitting the SE parameters to Tauc-Lorentz oscillators. The composition of the film was determined using X-ray photoelectron spectroscopy (XPS). The structural properties of the thin films were studied using grazing incidence x-ray diffraction (GIXRD) with a fixed omega value of 5°. Transmission (T) and reflection (R) were measured with a PerkinElmer Spectrophotometer (LAMBDA1050 UV/Vis/NIR) and absorption (A) was calculated assuming A+R+T = 1. The photoluminescence spectrum was recorded using a Renishaw inVia Qontor spectrometer with an excitation laser wavelength of 325 nm. Phonon properties were measured in a Renishaw inVia Reflex Raman spectrometer with a 532 nm laser.

3. Results

3.1. Structural characterization

Fig. 1 shows the X-ray diffractogram of an as-deposited hafnium oxynitride film and after different annealing temperatures and time. Unlike previously reported observations, the as-deposited film was partially annealed as evident from the presence of {222}, {004} and {71−2} peaks [7,20]. At a very high temperature of 800 °C and above all the characteristic peaks of hafnium oxynitride have appeared. Similar trends have been observed before, where higher nitrogen content in the lattice pushed the crystallization temperatures to higher values [20]. With the increase in annealing temperature to 800 °C and beyond, additional crystallization planes have started to appear. The film crystallized at 850 °C shows sharp and distinct peaks corresponding to the cubic (γ) or monoclinic (m) phase of hafnium oxynitride, but film annealed at a temperature higher than 850 °C shows the oxygen-rich phases of hafnium oxynitride evident from a shift of 2θ to lower values. Additionally, films annealed at these high temperatures also show characteristic peaks for HfO_2. In Table 1 the literature and experimental 2θ values and the corresponding plane of reflection for the various phases of Hf_2ON_2 are presented. The 2θ peak positions for experimentally grown thin film and annealed at 850 °C for 60 s match very closely to the literature values corresponding to cubic or monoclinic Hf_2ON_2. In Fig. 1(a) the peak positions corresponding to cubic and monoclinic phases have been marked as dashed lines in orange and sea-green colours respectively. The peak positions for the sample annealed at 850 °C or below match well with the cubic (ICDD Card No: 00-050-1171) and monoclinic phase [25]. Whereas the peaks for the sample annealed at temperatures higher than 850 °C match well with the hexagonal phase (an oxide-rich phase) (ICDD Card No: 00-050-1173).

Fig. 1(b) shows the results of XRD measurements on the sample annealed at 850 °C for different durations. We observe that almost all the significant peaks corresponding to the cubic or monoclinic phase start to appear after annealing for 15 s. The peaks get sharper in intensity for annealing up to 60 s, with a shift in peak position at higher annealing durations where the intensity also appears to decrease.

The crystallite size in the samples annealed at 850 °C for the 60 s (γ/m phase), calculated using Scherrer’s equation, is shown in Table 1. The value of the shape factor used was 0.9 as the exact crystallite shape is unknown. The value of the crystal size calculated from different peaks are in the range of 3.36 nm to 7.85 nm. This variation could be attributed to the presence of mixed phases where crystallization properties for each of the phases are different. The last column of Table 1 shows the

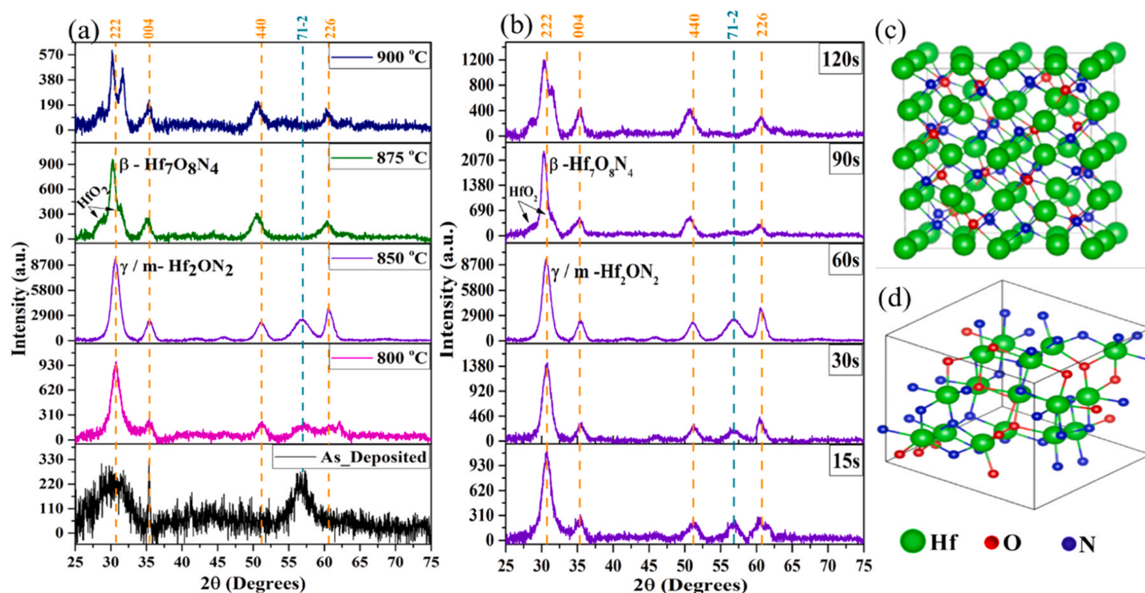

Fig. 1. Results of X-ray diffraction measurements of a Hafnium oxynitride thin film on Si substrate: (a) Dependence on RTA temperature for 60 s anneals, (b) Dependence on RTA Time for 850 °C anneals. The orange and sea-green colour dashed lines correspond to the 2θ values for cubic and monoclinic phases of Hf_2ON_2 respectively, and (c-d) Crystal structures for cubic and monoclinic phases of Hf_2ON_2 respectively [15,25].

Table 1
Literature values for major 2θ peaks and corresponding planes of reflection for different phases of Hafnium oxynitride. Experimental values are for a thin film synthesized in this work.

Literature						*Experimental*			
Cubic		*Monoclinic*		*Hexagonal*				*Crystallize size (D)*	*Average D*
2θ	*{hkl}*	*2θ*	*{hkl}*	*2θ*	*{hkl}*	*2θ*	*{hkl}*	-	-
30.75	{222}	30.65	{111}	30.51	{3−11}	30.71	{222}	6.87 nm	**6.47 nm**
35.65	{004}	33.94	{310}	35.38	{3−22}	35.54	{004}	7.13 nm	
51.31	{440}	50.91	{313}	50.88	{214}	51.25	{440}	6.81 nm	
61.03	{226}	56.86	{71−2}	50.91	{410}	56.86	{71−2}	3.68 nm	
-	-	58.63	{711}	60.50	{5−43}	60.95	{226}	7.85 nm	

average of the 6 values of the crystallize size given in the previous column. The thickness of as-deposited film on quartz substrate reduced from 86 nm to 41.02 nm after RTA at 850 °C for 60 s measured using a Dektak surface profiler. The value for thickness was also confirmed by fitting the ellipsometry data where the thickness extracted was 41.02 nm. This reduction in thickness after RTA is consistent with previously reported observations [15]. Such a strong reduction in films thickness suggests reduction in the pores or increase in density of the films.

3.2. Chemical state analysis

The result of the XPS depth profile on a hafnium oxynitride film is shown in Fig. 2. In Fig. 2(a), we can see two distinct low and high-energy doublets of Hf4f peaks in both the core and at the surface of the film. The low energy doublet occurring at 15.42 eV and 17.03 eV ($Hf4f_{7/2}$ and $Hf4f_{5/2}$) is assigned to the metallic nature of Hf-N. Similar binding energy for the low energy Hf4f doublet has been reported in [22] for non-stoichiometric $HfN_{0.19}$. The high-energy doublet occurs at binding energies 16.74 and 18.41 eV ($Hf4f_{7/2}$ and $Hf4f_{5/2}$) which match the values reported in [23]. The peak positions shift to higher energy at the surface owing to the formation of Hf-O bonds. However, these energies are lower compared to HfO_2 energies because of nitrogen incorporation in the lattice. The binding energies for Hf4f in HfO_2 are reported to be 19.2 eV and 17.5 eV for $Hf4f_{5/2}$ and Hf 4 $f_{7/2}$, respectively [20]. We find energy significantly lower than these both at the surface and in the bulk of the film. The binding energy of N1s in the core has asymmetric peaks at 396.56 eV and 398.52 eV as shown in Fig. 3(b). Similar peak positions have been reported in [23] where they assign the peaks to Hf–N–Hf and Hf–N–O bonds. The O1s binding energy in the core is centred around 531.13 eV which matches the value reported in the reference [23] and has been assigned to Hf–N–O.

The binding energies for O^{2-} species centre around 530.1 eV which is absent here in the core suggesting an absence of HfO_2 bonds [26]. The XPS spectrum shows the presence of carbon impurities in the core as well. C1s peak is present at a binding energy 282.27 eV which matches with the value for HfCx reported earlier for ALD deposited samples using TEMAHf as hafnium precursor [2,15]. Overall, the films show Hf-N-O in the core and Hf-O-N at the surface. The ALD-deposited samples were taken out of the N_2 chamber for XPS measurements. The surface of the films is likely to get oxidized where some of the N_2 bonded to hafnium were replaced by O_2. The chemical states of the elements in the core were measured after etching the film to 15 nm from the surface. In terms of optical properties, oxygen bonded to nitrogen will increase the band gap of the material towards HfO_2 (Insulator). And nitrogen bonded to Hf will reduce the band gap of the material towards HfN (Metallic). From a hot carrier solar cell perspective, it is advantageous to have nitrogen bonded to hafnium to have semiconducting properties from the thin films.

3.3. Optical properties

Absorption (A), transmission (T), and reflection (R) spectra of the sample annealed at 850 °C for 60 s are shown in Fig. 3(a). The film

Fig. 2. XPS spectrum of Hf4f, N1s, O1s and C1s elements in the thin Hafnium oxynitride films. Solid circles denote the binding energy for the elements at any depth in the film and open circles at the surface. The chemical states of the elements were studied using a mono-chromated Al K-Alpha X-Ray source (1486.68 eV) after etching the films for about 15 nm.

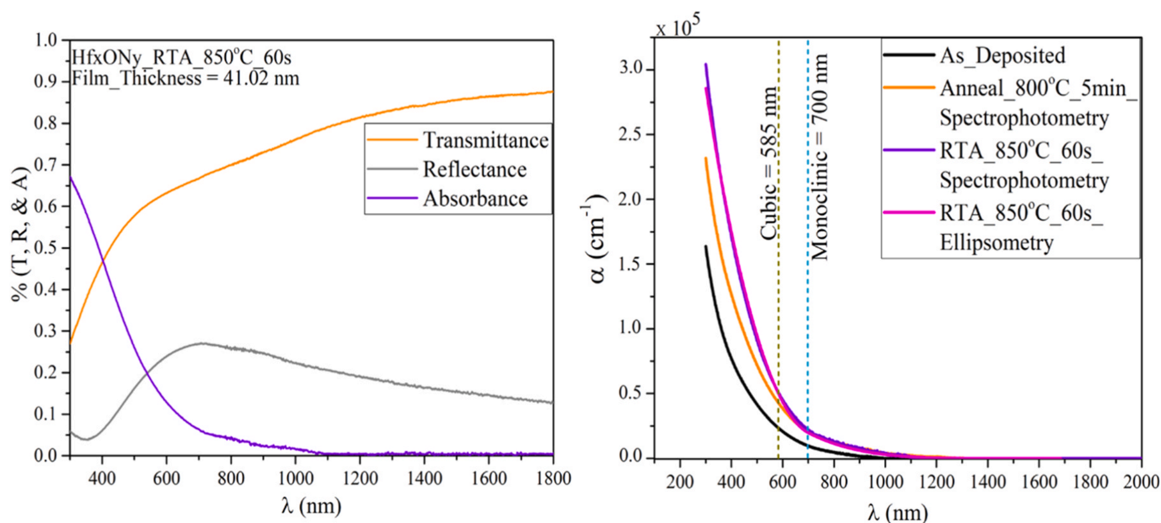

Fig. 3. (a) Transmittance, Reflectance and Absorbance of hafnium oxynitride thin films on a quartz substrate. (b) Absorption coefficients of as-deposited and annealed samples. The dashed lines represent the theoretical simulated electronic band gaps of hafnium oxynitride.

shows a substantial increase in reflection from the infrared to the visible region with a peak closer to 709.43 nm. This suggests the onset of the Fermi region which usually has high electron density where reflections of light increase because of scattering of light. Also, the absorbance of the film increases monotonously from around 710.39 nm which resembles a band gap region for semiconductors. The absorption coefficients (α) of the films were calculated using the following expression [15,27]:

$$\alpha_{film} = (\frac{dsub}{dtot}) * (\frac{1}{dfilm}) * \ln(\frac{1 - Rtot}{Ttot}) - (\frac{1}{dfilm}) * \ln(\frac{1 - Rsub}{Tsub}) \quad (1)$$

Where, d denotes thickness and subscripts *tot*, *sub*, *film* refers to thin film on the substrate, only substrate and only thin film.

The absorption coefficients of the samples increased exponentially after RTA and standard furnace annealing from around 710 nm (Fig. 3(b)). The as-deposited sample also shows very strong absorption around the same range. One possible reason could be the partial annealing of the sample by the plasma exposure during its synthesis where the films crystallized in some preferred directions. The theoretical band gap for cubic (585 eV) and monoclinic (700 eV) phases of Hafnium oxynitride are marked by dashed-green and dashed-cyan lines, respectively, in Fig. 3(b) [15,25]. The onset of exponential absorption matches very closely with the theoretical band gap of the monoclinic phase. However, the absorption onset of the as-deposited sample partially matches both theoretical values. The substantial absorption in all the samples before the onset of the absorption edge, commonly referred to as Urbach Tail suggests the presence of defect states in the films [7]. The defects create additional energy levels in the band gap of hafnium oxynitride (HfON) films thus reducing the actual band gap of HfON. These energy levels also act as trap states for the charge carriers which is not beneficial for applications that require sharp and defined band gaps [7,28]. In this case, the absorption does not drop to zero below the band gap energy but shows some absorption beyond the band gap edge suggesting the presence of some carbides which is also evident from the XPS results. PL spectrum from the as-deposited and annealed samples are shown in Fig. 4. Emission close to 570 nm and around 704.78 nm can be observed, which matches with theoretical band bag value for cubic and monoclinic phases, respectively. The PL intensity has increased with annealing temperature and annealing duration. The RTA sample for the 30 s shows relatively sharper absorption peaks at 576.72 nm. The peak at 576.72 nm broadens and intensity decreases after annealing for 60 s. The peak intensity at 704.78 nm increases with annealing. This behaviour was also observed in the XRD diffractogram where the (71−2) planes corresponding to the monoclinic phase became sharp and distinct after annealing for 60 s.

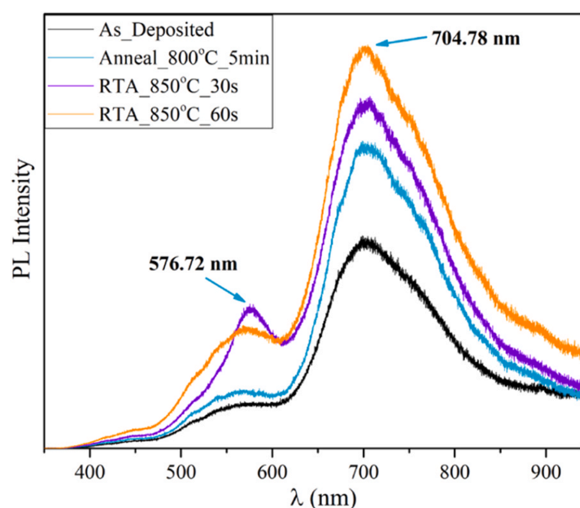

Fig. 4. PL spectrum from the as-deposited and annealed Hafnium oxynitride films. The films show a sharp absorption at 704.78 nm and broad absorption around 576.72 nm.

The optical constants, complex refractive indices, reflection, transmission spectrum etc. of thin films can be extracted from either of the two expressions: Complex Refractive Index $(\tilde{n}(\lambda) = n(\lambda) + ik(\lambda))$ or Complex Dielectric Function $(\varepsilon(\lambda) = \varepsilon_1(\lambda) + i\varepsilon_2(\lambda))$ [29]. The former describes how material impacts the light wave, and the latter describes how the wave affects the materials. Both expressions constitute two constants, first as real and second as imaginary, with the real part to study refractive index and the imaginary part to study attenuation. Spectroscopic ellipsometry (SE) parameters Ψ and Δ of Hafnium oxynitride on quartz substrate have been plotted in Fig. 5(a) and Fig. 5(b) with SE model fitting. The experimental values of Ψ and Δ were determined by a fit using two Tauc-Lorentz (TL) oscillators with a mean squared error of 1.499 as reported in the reference [30,31]. As can be seen the model fits the experimental data accurately.

The wavelength-dependent refractive index (n) and extinction coefficient (k), extracted from Ψ and Δ are plotted in Fig. 5(c). The extinction coefficient decays until around 692.54 nm (1.79 eV) where the rate of change becomes smaller. The value of k reduces to zero value around 1300 nm (0.95 eV). Wavelength (λ) dependent absorption coefficient (α) was calculated from extinction coefficient (k) using the following expression [[32]:

$$\alpha = \frac{4 * pi * k}{\lambda} \quad (2)$$

The α extracted from SE matches perfectly with the absorption coefficient calculated from spectrophotometry (see Fig. 3(b)). This validates the use of the SE model to fit the experimental Ψ and Δ parameters and gives confidence in the extracted n & k values. In a standard SE data fitting, ε_i is fitted first and then ε_r is calculated from the Kramers – Kronig relationship. ε_r and ε_i were extracted directly from the Complete Ease software which by default implements the Kramers – Kronig relationship (Fig. 5d). The extracted components of the dielectric constants follow a similar trend to the n & k values.

3.4. Raman properties

Fig. 6 shows the Raman spectrum of the hafnium oxynitride thin films deposited on Si and Quartz substrates. The measured Raman spectrum for the RTA samples at 850 °C and furnace-annealed samples at 800 °C agrees very closely with the theoretically simulated phonon band structure as reported in [15]. The theoretical phonon band gap for γ-Hf_2ON_2 does not appear between acoustic phonons (AP) and optical phonons (OP). But it has been reported between 250 and 275 cm^{-1} all in the OP range. We find negligible phonon states between 242 and 265 cm^{-1} and 235–263 cm^{-1} in the quartz and Si substrates respectively. The acoustic phonons are very small in magnitude and whatever appears is mostly because of the folding of the AP as the films are 41.02 nm. The Raman spectrum for the samples annealed for 5 mins at 800 °C showed very clear and distinct AP and OP states. The sharp dip in the OP intensities close to 525 cm^{-1} in the Si substrate could be because of the matching of the phonon states of the Si substrate and the Hafnium oxynitride film. The Raman spectrum for the samples annealed at both rapid and slow rates show similar phonon profiles. However, the films with RTA for the 60 s show smaller intensities compared to the 30 s. This was probably because of the change in the mixed crystal structure of the films evident from the XRD studies. We also observe a dip in the OP intensities from 506 to 575 cm^{-1} which do not match with the theoretical cubic phonon frequencies. It has been reported that the phonon states change drastically with changes in substrate [10]. However, we find a very similar spectrum irrespective of the substrate suggesting similar crystal quality on both Si and Quartz. The Raman phonon frequencies for HfO_2 centres around 140–200 cm^{-1} and 500 cm^{-1}. We find absence of these phonon frequencies in the Raman spectrum suggesting absence of HfO_2 phases matching very well with the XPS study.

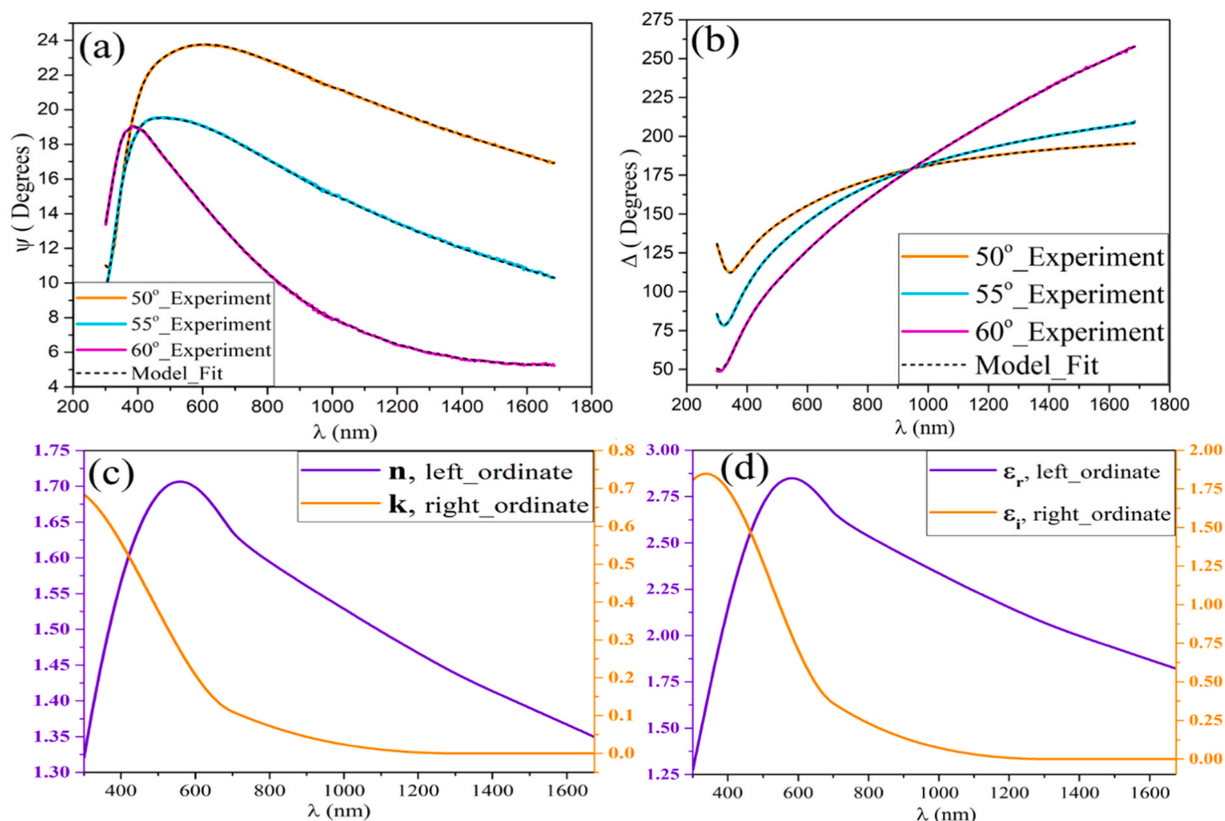

Fig. 5. Experimental and model fit data for SE parameters a) Ψ and b) Δ at 50°, 55° and 60° angle of incidence. c) Refractive index (n) and extinction coefficients (k) of the hafnium oxynitride films. d) Real and Imaginary components of the dielectric constants of the hafnium oxynitride.

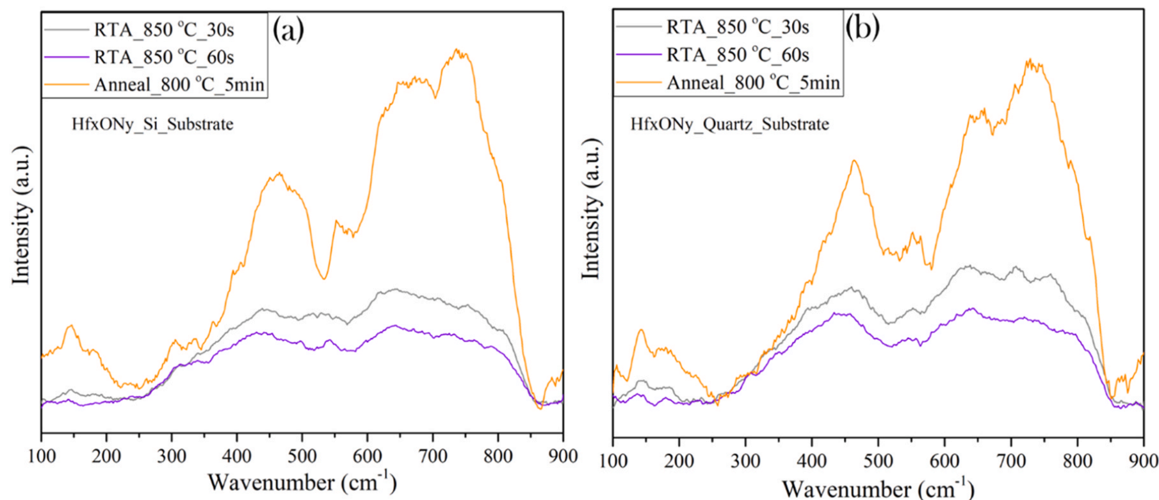

Fig. 6. Raman spectrum of hafnium oxynitride thin films on Si and Quartz substrates with an excitation wavelength of 532 nm.

4. Discussion

The as-deposited films showed partial crystallisation. The crystallization of the thin films improved significantly after annealing at a temperature close to 850 °C evident by the presence of characteristic peaks of Hf_2ON_2. The films annealed at higher than 850 °C showed oxide-rich phases which is consistent with previously reported values [8]. Also, films annealed for a shorter duration lacked sufficient time for crystallization and a longer annealing duration revealed oxide phases evident from the XRD diffractogram. So, annealing the films at 850 °C for 30–60 s seems to be beneficial from an HCSC perspective as oxide rich phase is detrimental to the application. The Hafnium oxynitride films have crystallized in mixed cubic and monoclinic phases. These observations also align very closely with the optical properties (Spectrophotometry, SE, and PL) which show strong absorption from ~ 710 nm. From the SE model fitting, the band gap energy for the Tauc-Oscillators is very close to 1.74 eV (712 nm). Also, the absorption coefficient from spectrophotometry and SE shows an exponential increase from 710 nm which coincides with the monoclinic phase. The PL spectrum shows the presence of two band gaps (around 575 nm and 700 nm, see Fig. 4) which are very close to the theoretical band gap of cubic and monoclinic phases, respectively. Density functional theory

typically underestimates the band gaps of materials. However, the use of hybrid and meta-generalized gradient approximation (mGGA) functionals has been shown to more precisely predict band gap energies [33]. The theoretical band gap obtained using mGGA functionals matches very closely with the experimental band gap energies of the hafnium oxynitride synthesized in this work. The peak intensity corresponding to the cubic phase is sharply pronounced for the sample annealed at 850 °C for 30 s. The intensity for the cubic phase decreases with annealing for 60 s and instead, the intensity increases for the monoclinic phase. This observation is very consistent with the XRD results which showed sharp and distinct monoclinic peaks when the RTA time increased from 30 s to 60 s at 850 °C. Overall, the properties of the thin films are more influenced by the monoclinic phase for the samples with RTA at 850 °C for 60 s.

The SE results show a change of peak profile in the refractive index for the Hafnium oxynitride thin films on quartz substrate from around 707.84 nm. This suggests the presence of high electron density at these energy levels which is a typical characteristic for Fermi levels. This suggests the onset of a band gap region in the Hafnium oxynitride films which coincides with the monoclinic phase. The presence of the cubic phase is also confirmed by the Raman spectra where the phonon band gap of the experimental data coincides with the estimated theoretical phonon band gap [15]. However, the decrease in intensity of the phonon frequencies around 506–575 cm^{-1} is still unclear and most probably related to the monoclinic phase of hafnium oxynitride. The Raman spectrum shows a low density of acoustic phonon states which are beneficial from a HCSC perspective. This is because a lower acoustic phonon density of states will provide limited decay paths for the optical phonons to acoustic phonons hence slowing down the hot carrier cooling rate [34,35]. This is important for hot carrier solar cells as their efficiency is strongly dependent on the hot carrier cooling rate [36]. A lower acoustic phonon density also enhances the possibility of achieving a phonon bottleneck effect at a lower phonon excitation intensity. Attempt to determine acoustic impedance through the measurement of the coherent acoustic phonon velocity of the films using Eq. (3) [15] was not successful. Because of the poor signal quality in terms of defined phonon oscillations in the infrared region, the Fourier transform of the Transient absorption spectrum data was not possible due to missing data points at some required wavelengths (See Supplementary information S1). The work is in progress for the optimization of the laser system to extract a uniform spectrum. Alternative methods of mechanically measuring the sound velocity are also being investigated. The films are highly absorbing in the visible spectrum which widens its application to various photo-electronics applications. Based on the results of XRD, UV–visible spectrophotometry, spectroscopic ellipsometry and the Raman spectra, the stoichiometry of the thin films is expected to be Hf_2ON_2.

$$v = \frac{f * \lambda}{2 * n} \quad (3)$$

Where ν is the acoustic wave velocity, f is the Coherent Acoustic Phonon frequency extracted after the Fourier transform of the transient absorption spectrum, λ is the wavelength of the probe, and n is index of refraction of the thin film.

5. Conclusions

In conclusion, thin films of hafnium oxynitride were deposited on Si and quartz substrate through the plasma-enhanced ALD process. The presence of mixed-phase (cubic and monoclinic) in hafnium oxynitride was reported by XRD, optical and Raman results, with the crystallization strongly dependent on annealing temperature and time. The films showed PL peaks close to 705 nm and 575 nm which are consistent with the theoretical reported values. This is the first report on the PL and Raman spectrum of a single-standing thin film of hafnium oxynitride. The hafnium oxynitride films show strong absorption in the visible spectrum with the absorption tail decaying close to 1300 nm. Significant absorption before the absorption edge suggests the presence of defect states, commonly described as Urbach's tails. The measured Raman spectrum matches well with the theoretically modelled phonon dispersion for cubic Hf_2ON_2. The results of the spectroscopic ellipsometry also suggested semiconducting behaviour matching very closely the results from spectrophotometry. Overall, the hafnium oxynitride thin films look very promising for application as HCSC absorbers from the semiconductor's perspective because of its absorption, PL, and phonon spectrum. However, the suitability of hafnium oxynitride as a HCSC absorber has yet to be established and HCSC properties, such as lifetime, thermalisation rates etc. of hafnium oxynitride thin films are the subject of ongoing research.

CRediT authorship contribution statement

Gavin Conibeer: Funding acquisition, Resources, Supervision, Validation, Writing – review & editing. **Santosh Shrestha:** Funding acquisition, Resources, Supervision, Validation, Writing – review & editing. **Ayush Pratik:** Conceptualization, Data curation, Formal analysis, Investigation, Methodology, Validation, Visualization, Writing – original draft, Writing – review & editing. **Robert Patterson:** Formal analysis, Validation, Writing – review & editing.

Declaration of Competing Interest

The authors declare that they have no known competing financial interests or personal relationships that could have appeared to influence the work reported in this paper.

Data availability

Data will be made available on request.

Acknowledgement

This research was supported by the Australian Government through the Australian Research Council's Discovery Projects funding scheme (project DP170102677). The authors acknowledge the staff at Mark Wainwright Analytical Centre at the University of New South Wales for their help and technical support.

Appendix A. Supporting information

Supplementary data associated with this article can be found in the online version at doi:10.1016/j.jallcom.2024.173925.

References

[1] U. Sharma, G. Kumar, S. Mishra, R. Thomas, Advancement of gate oxides from SiO2 to high-k dielectrics in microprocessor and memory, J. Phys. Conf. Ser. vol. 2267 (1) (2022) 1–7, https://doi.org/10.1088/1742-6596/2267/1/012142.
[2] S. Consiglio, W. Zeng, N. Berliner, E.T. Eisenbraun, Plasma-assisted atomic layer deposition of conductive hafnium nitride using tetrakis(ethylmethylamino) hafnium for CMOS gate electrode applications, J. Electrochem Soc. vol. 155 (3) (2008) H196, https://doi.org/10.1149/1.2827995.
[3] Y. Zhang, J. Lu, K. Onodera, R. Maeda, Development of hafnium oxynitride dielectrics for radio-frequency-microelectromechanical system capacitive switches, Sens Actuators A Phys. vol. 139 (1-2) (2007) 337–342, https://doi.org/10.1016/j.sna.2007.02.005.
[4] W. Zhu, et al., HfO2 and HfAlO for CMOS: Thermal stability and current transport, Tech. Dig. Int Electron Devices Meet. (2001) 463–466, https://doi.org/10.1109/iedm.2001.979541.
[5] M. Chisaka, H. Sasaki, H. Muramoto, Monoclinic hafnium oxynitride supported on reduced graphene oxide to catalyse the oxygen reduction reaction in acidic media† (0) (2014) 20415–20419, https://doi.org/10.1039/c4cp03210a.
[6] A.P. Black, et al., New rare earth hafnium oxynitride perovskites with photocatalytic activity in water oxidation and reduction, Chem. Commun. vol. 54 (12) (2018) 1525–1528, https://doi.org/10.1039/c7cc08965a.

[7] B. Thapa, M. Dubajic, G. Conibeer, S. Shrestha, Synthesis and characterisation of hafnium oxynitride thin film: can it be used as a hot carrier solar cell material? Conference Record of the IEEE Photovoltaic Specialists Conference (2021) 1654–1658, https://doi.org/10.1109/PVSC43889.2021.9518501.

[8] B. Thapa, R. Patterson, M. Dubajic, G. Conibeer, S. Shrestha, Investigation of structural and optical properties of atomic layer deposited hafnium nitride films, Conf. Rec. IEEE Photovolt. Spec. Conf. (2019) 1797–1801, https://doi.org/10.1109/PVSC40753.2019.8980718.

[9] S. Shrestha, et al., Potential of HfN, ZrN, and TiH as hot carrier absorber and Al2O3/Ge quantum well/Al2O3 and Al2O3/PbS quantum dots/Al2O3 as energy selective contacts, Jpn. J. Appl. Phys. vol. 56 (8) (2017), https://doi.org/10.7567/JJAP.56.08MA03.

[10] S. Chung, et al., Hafnium nitride for hot carrier solar cells, Sol. Energy Mater. Sol. Cells vol. 144 (2016) 781–786, https://doi.org/10.1016/j.solmat.2014.10.011.

[11] H. Xia, et al., Hot carrier dynamics in HfN and ZrN measured by transient absorption spectroscopy, Sol. Energy Mater. Sol. Cells vol. 150 (2016) 51–56, https://doi.org/10.1016/j.solmat.2016.01.026.

[12] G.J. Conibeer, D. König, M.A. Green, J.F. Guillemoles, Slowing of carrier cooling in hot carrier solar cells, Thin Solid Films vol. 516 (20) (2008) 6948–6953, https://doi.org/10.1016/j.tsf.2007.12.102.

[13] Y. Zhang, C. Huang, Study the mechanisms of enhanced phonon bottleneck effect for the absorber of hot carrier solar cell in III-V multiple quantum wells, IOP Conf. Ser. Mater. Sci. Eng. vol. 774 (1) (2020), https://doi.org/10.1088/1757-899X/774/1/012127.

[14] Y. Zhang, L. Tang, B. Zhang, P. Wang, C. Xu. Quantitative study on the mechanisms underlying the phonon bottleneck effect in InN / InGaN multiple quantum wells, vol. 103104, 2020, pp. 1–5, http://10.1063/5.0003201.

[15] R.E. Engineering, Nitrides and Oxynitrides of Hafnium and Zirconium: Simulation, Synthesis and Characterisation from the Hot Carrier Solar Cell Perspective Bharat Thapa, no. September, 2021.

[16] D.I. Bazhanov, A.A. Knizhnik, A.A. Safonov, A.A. Bagatur'yants, M.W. Stoker, A. A. Korkin, Structure and electronic properties of zirconium and hafnium nitrides and oxynitrides, J. Appl. Phys. vol. 97 (4) (2005), https://doi.org/10.1063/1.1851000.

[17] M. DeMiguel-Ramos, et al., Hafnium nitride as high acoustic impedance material for fully insulating acoustic reflectors. IEEE International Ultrasonics Symposium (IUS), Kobe, Japan, 2018, pp. 1–4, 10.1109/ULTSYM.2018.8579935.

[18] G. Conibeer, et al., Progress on hot carrier cells, Sol. Energy Mater. Sol. Cells vol. 93 (2009) 713–719, https://doi.org/10.1016/j.solmat.2008.09.034.

[19] G. Conibeer, et al., Hot carrier solar cell absorbers: materials, mechanisms and nanostructures, Next Generation Technologies for Solar Energy Conversion V vol. 9178 (2014) 917802, https://doi.org/10.1117/12.2067926.

[20] Y.B. Lee, I.K. Oh, E.N. Cho, P. Moon, H. Kim, I. Yun, Characterization of HfO x N y thin film formation by in-situ plasma enhanced atomic layer deposition using NH 3 and N 2 plasmas, Appl. Surf. Sci. vol. 349 (2015) 757–762, https://doi.org/10.1016/j.apsusc.2015.05.066.

[21] J.Y. Wu, Y.T. Chen, M.H. Lin, T.B. Wu, Ultrathin HfON trapping layer for charge-trap memory made by atomic layer deposition, IEEE Electron Device Lett. vol. 31 (9) (2010) 993–995, https://doi.org/10.1109/LED.2010.2052090.

[22] C.S. Kang, et al., Bonding states and electrical properties of ultrathin HfOxN y gate dielectrics, Appl. Phys. Lett. vol. 81 (14) (2002) 2593–2595, https://doi.org/10.1063/1.1510155.

[23] P. Lei, et al., Enhanced mechanical properties of HfO2 film by nitrogen doping, Surf. Eng. vol. 32 (8) (2016) 585–588, https://doi.org/10.1080/02670844.2015.1121342.

[24] V. Dave, P. Dubey, H.O. Gupta, R. Chandra, Microstructural and optical properties of Sputter deposited Hafnium oxynitride films on glass substrate, 2013 International Conference on Energy Efficient Technologies for Sustainability, ICEETS 2013 (2013) 1031–1035, https://doi.org/10.1109/ICEETS.2013.6533528.

[25] T.M. Project, The Materials Project. Materials Data on Hf2N2O by Materials Project. United States. Lawrence Berkeley National Lab. (LBNL), Berkeley, CA (United States). LBNL Materials Project. http://doi.org/10.17188/1291559.

[26] X. Yang, et al., Nitrogen-plasma treated hafnium oxyhydroxide as an efficient acid-stable electrocatalyst for hydrogen evolution and oxidation reactions, Nat. Commun. vol. 10 (1) (2019) 1–8, https://doi.org/10.1038/s41467-019-09162-5.

[27] S. Chung, Hot Carrier Solar Cells: Hafnium Nitride as an Absorber Material, no. March, 2017, [Online]. Available: http://unsworks.unsw.edu.au/fapi/datastream/unsworks:43364/SOURCE02?view=true.

[28] H.P. Piyathilaka, et al., Hot-carrier dynamics in InAs/AlAsSb multiple-quantum wells, Sci. Rep. vol. 11 (1) (2021) 1–8, https://doi.org/10.1038/s41598-021-89815-y.

[29] D.B. Tanner, The Complex Dielectric Function and Refractive Index, Opt. Eff. Solids (2019) 17–29, https://doi.org/10.1017/9781316672778.004.

[30] T. Tan, Z. Liu, H. Lu, W. Liu, H. Tian, Structure and optical properties of HfO2 thin films on silicon after rapid thermal annealing, Opt. Mater. (Amst.) vol. 32 (3) (2010) 432–435, https://doi.org/10.1016/j.optmat.2009.10.003.

[31] D. Saha, et al., Spectroscopic ellipsometry characterization of amorphous and crystalline TiO 2 thin films grown by atomic layer deposition at different temperatures, Appl. Surf. Sci. vol. 315 (1) (2014) 116–123, https://doi.org/10.1016/j.apsusc.2014.07.098.

[32] H.J. Lee, M.M.A. Gamel, P.J. Ker, M.Z. Jamaludin, Y.H. Wong, J.P.R. David, Absorption coefficient of bulk III-V semiconductor materials: a review on methods, properties and future prospects, J. Electron. Mater. vol. 51 (11) (2022) 6082–6107, https://doi.org/10.1007/s11664-022-09846-7.

[33] A.J. Garza, G.E. Scuseria, Predicting band gaps with hybrid density functionals, J. Phys. Chem. Lett. vol. 7 (20) (2016) 4165–4170, https://doi.org/10.1021/acs.jpclett.6b01807.

[34] Y. Zhang, et al., A review on thermalization mechanisms and prospect absorber materials for the hot carrier solar cells, Sol. Energy Mater. Sol. Cells vol. 225 (no.) (2021) 111073, https://doi.org/10.1016/j.solmat.2021.111073.

[35] S. Kahmann, M.A. Loi, Hot carrier solar cells and the potential of perovskites for breaking the Shockley-Queisser limit, J. Mater. Chem. C Mater. vol. 7 (9) (2019) 2471–2486, https://doi.org/10.1039/c8tc04641g.

[36] G. Conibeer, Y. Zhang, S.P. Bremner, S. Shrestha, Towards an understanding of hot carrier cooling mechanisms in multiple quantum wells, Jpn. J. Appl. Phys. vol. 56 (9) (2017), https://doi.org/10.7567/JJAP.56.091201.